Bayesian Intention Inference for Trajectory Prediction with an Unknown Goal Destination

Graeme Best and Robert Fitch

***Abstract*— Contextual cues can provide a rich source of information for robots that operate in the presence of other agents such as people, animals, vehicles and fellow robots. We are interested in context, in the form of the behavioural intent of an agent, for enhanced trajectory prediction. We present a Bayesian framework that estimates both the intended goal destination and future trajectory of a mobile agent moving among multiple static obstacles. Our method is based on multi-modal hypotheses of the intended goal, and is focused primarily on the long-term trajectory of the agent. We propose a computationally efficient solution and demonstrate its behaviour in a pedestrian scenario with a real-world data set. Results show the benefits of our method in comparison to traditional trajectory prediction methods and illustrate the feasibility of integration with higher-level planning algorithms.**

I. Introduction

A wide variety of application areas such as agriculture, defence and domestic service involve robots that must operate alongside people, animals, human-driven vehicles and other robots. One core capability of these robots is to be able to predict the future trajectories of fellow moving agents [2], [1], [6], [9], [13], [3], at a minimum for implementing successful collision avoidance. Incorrect predictions can result in collisions while imprecise predictions can impact the robot's ability to satisfy its primary objectives. We are interested in exploiting the context of the application, in the form of the agent's *intent*, to improve trajectory prediction.

Models that predict the motion of dynamic agents critically rely on contextual assumptions. Examples of common simple assumptions include near-constant velocity or acceleration [6] and predefined trajectories [3]. However these simple assumptions can lead to weak predictors in complex environments populated by many obstacles and unknown factors that may influence the agent's short-term behaviour. More complex contextual assumptions, such as the agent's intent, allow for reasoning about the interaction between the agent and its environment over a long time period and thus can lead to more robust predictors.

In this work we consider the case where an agent is driven by the high-level intention to move to some unknown goal region within a cluttered environment, and is rational in the sense that it aims take a short path. This case occurs in many scenarios such as pedestrians walking through a train station or robots delivering packages. The agent's intention is initially unknown, but can be estimated given previous observations of the agent's motion and a map of the environment. An example is shown in Fig. 1. The challenge is how to develop a probabilistic formulation of this estimation problem along with computationally efficient solutions.

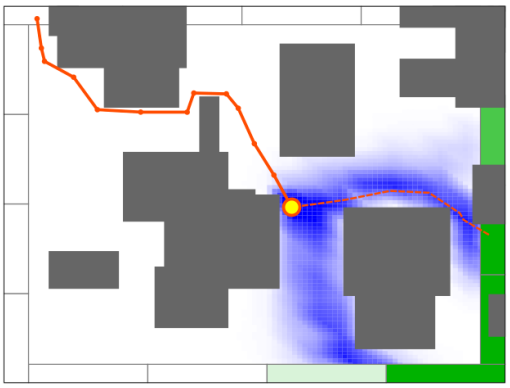

Fig. 1. Example agent (orange) moving through an environment with static obstacles (grey), from top left to the centre. The algorithm predicts it will next move to the right or downwards with some probability (blue). The intended goal is estimated to most likely be one of the darker green regions at the bottom right.

We approach the trajectory prediction problem using a novel mathematical formulation that first estimates the agent's intention and then uses the resulting probability distribution to predict the position of the agent in the future. Central to our formulation is a probabilistic dynamics model that is used to compute a probability distribution representing the next position of the agent conditional on the current position and intention. The intention inference phase employs a Bayesian estimation framework that can be computed efficiently. The trajectory prediction phase extrapolates the agent's position recursively, but is difficult to solve analytically. We therefore propose a probabilistic roadmap discretisation of the environment and a Monte-Carlo sampling technique that converges to the true predictive distribution as more sample paths are drawn. We show empirically that the technique converges with few samples and performs efficiently in practice.

We demonstrate the behaviour of our algorithms in the scenario of predicting paths of pedestrians moving through a busy environment, using a real-world dataset with 442 pedestrian trajectories. Results show that our method results in high accuracy and prediction certainty compared to a method that does not consider the intention of the agent. Our results also demonstrate the feasibility of our method for integration with collision avoidance and other types of planning algorithms.

The authors are with the Australian Centre for Field Robotics (ACFR), The University of Sydney, Sydney, Australia. {g.best,rfitch}@acfr.usyd.edu.au

II. Related Work

Approaches to the trajectory prediction problem largely depend on the underlying assumptions about the motion of the agent or object of interest. The simplest assumption is that the agent is stationary, which may be appropriate for some applications [16].

Another simple assumption is that the agent will continue moving with constant or near-constant velocity or acceleration [6], [12]. These assumptions allow for efficient computation and may be a sufficient prediction model to improve performance in tracking applications. However these simple models are often insufficient for dynamic collision avoidance applications where performance is highly dependent on the accuracy of the predictions rather than the accuracy of the current position estimate, particularly when extrapolating relatively far into the future.

Similar models can be extended to model multi-agent collision avoidance in crowds, which is a highly-active area of research [10], [11], [17], [14], [9]. However, due to the compounded uncertainty of crowds these predictions are usually only reliable in the very near future, while our focus is on longer term predictions.

Another common assumption is that the agent will reliably follow one of possibly many predefined paths that may come from training data based on previous agent trajectories [4], [1] or known mission plans [3]. For the case where there are multiple possible predefined paths, the predictions are characterised by a multi-modal distribution. Furthermore, the predictions can be improved by estimating which single paths out of all possible paths is the agent more likely to be following [4], [1]. The benefit of this approach is that any underlying assumptions about the agent's motion, such as probabilistic dynamics and velocity constraints, can be modelled implicitly within the predefined paths. However, most realistic scenarios are less predictable and therefore it is impractical to find a small discrete set of paths that accurately model the possible paths of the agent.

In this paper we reason over a potentially infinite number of paths that the agent could possibly take. However we group together all paths that have a common end position and then predictions are performed by first updating a belief for the end position of the agent's path. If the end position is known then this information can be used to improve the predictions [11]. However, in most cases the end position is not known and therefore it is advantageous to instead maintain a belief over all possible end positions based on observations or training data.

An agent moving through the environment is often guided by an underlying intention to move to another specific region of the environment. In this sense, each movement taken by the agent can be thought of as an action leading towards achieving the underlying intention to move to a goal region of the environment. This falls into the scope of *plan recognition* [5], [7]. General approaches to plan recognition are formulated around the idea that every observed action gives information about higher-level objectives, while reasoning over the higher-level objectives in turn gives information to predict future actions. Example applications of plan recognition in robotics includes robot table tennis, interactive humanoid robots [15] and inferring the plan of wheelchair operators [8].

The plan recognition concept has been used to formulate solutions to trajectory prediction problems. Some interesting proposed methods use a general definition of the agent's intention and therefore allow the use of more general frameworks such as POMDPs [2]. It can also be beneficial, and computationally efficient, to consider a more narrow definition of intention. Kim *et al.* [9] define the agent's intention to maintain a velocity close to an unknown preferred velocity which may change slowly over time as the agent moves through a crowd, using Kalman filters and a maximum-likelihood estimate of the model parameters. Schreier *et al.* [13] define intentions as typical manoeuvres while driving on structured roads, such as changing lanes, where inference is aided by observed properties of the road, such as the existence of lanes. We are interested in longer-term predictions where the underlying intention is to move to an unknown goal region within an environment of large static obstacles. In this case the direction may change rapidly even though the goal region is constant. Additionally, unlike in [9], we are interested in multi-modal belief distributions rather than a point estimate with uncertainty. We require this since, for example, the agent may move to the left or to the right of a large obstacle but cannot move through it.

III. Problem Formulation

In this paper we address the problem of predicting the future trajectory of an intelligent agent. We consider the case where the agent has a higher-level intention to move to a goal region of the environment, which is only known to the agent itself. The agent is assumed to take the shortest path to the goal region with some uncertainty while avoiding static obstacles.

More formally, at time t_i we seek to estimate the position X of the agent at time steps $t_{i+1}, t_{i+2}, ..., t_{i+k} := t_{i+1:i+k}$. The position estimates are described by the probability distributions $\Pr(X_{i+1}), \Pr(X_{i+2}), ..., \Pr(X_{i+k})$. The estimates are calculated based on the observed sequence of positions of the agent $x_1, x_2, ..., x_i$, and therefore is described by the conditional distribution $\Pr(X_{i+j} \mid X_{1:i} = x_{1:i})$.

The agent moves through a bounded environment Ψ that contains known static obstacles, (e.g., the grey obstacles in Fig. 1). The agent is assumed to navigate around the static obstacles and the set of all feasible positions of the agent is denoted $x_i \in \mathcal{X}$. For the sake of notation we assume the space $\mathcal{X}$ has been sufficiently discretised. The speed of the agent at time t_i is assumed to be drawn from a normal distribution with known parameters $|\dot{X}_i| \sim \mathcal{N}(\mu, \sigma^2)$. It is assumed that the agent is holonomic, however the proposed approach can be generalised for motion models of non-holonomic agents.

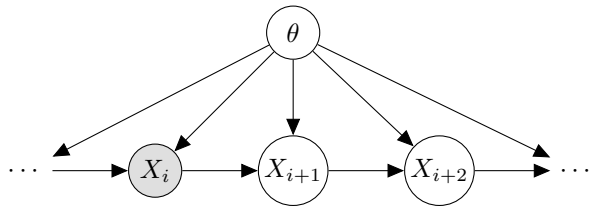

Fig. 2. Graphical model of the agent's trajectory. The previous and current positions $(X_1, X_2, ..., X_i)$ are fully observable, while the future positions $(X_{i+1}, X_{i+2}, ...)$ are to be predicted. The trajectory is conditional on the intention of the agent which is described by the latent variable θ.

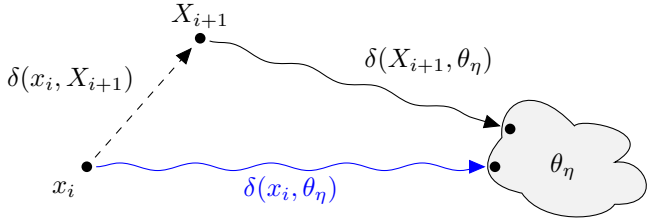

Fig. 3. Next position X_{i+1} along trajectory relative to the shortest path (blue) from the current position x_i to a known goal region θ_η. The new path distance is $\delta(x_i, X_{i+1}, \theta_\eta) = \delta(x_i, X_{i+1}) + \delta(X_{i+1}, \theta_\eta)$.

A. Intention of the Agent

The agent's trajectory is conditional on the intention of the agent which is only known to the agent itself. We describe this intention by the latent variable θ, and the trajectory of the agent is conditional on θ as depicted in Fig. 2. If θ is known precisely then this information can be used to give a more accurate estimate of the trajectory.

We assume that the agent's intention is to move along a path to a particular region θ within the environment. The goal region θ is one of finitely many predefined regions $\theta_1, \theta_2, ... \in \Theta$, such that each $\theta_\eta \subset \mathcal{X}$.

B. Probabilistic Dynamics Model

We assume that the agent will most likely take the shortest path to the goal region, with some uncertainty as described by the following transition model. The shortest path is calculated by taking into account the set of known static obstacles. We use $\delta(a, b)$ to denote the distance of the shortest path from position a to position or region b. Similarly, $\delta(a, b, c) = \delta(a, b) + \delta(b, c)$ denotes the distance of the shortest path from a to c that passes through b.

We define the probability distribution for the position at the next timestep as being exponential in the negative of the increase in the shortest path distance to a given goal θ_η:

$$\Pr(X_{i+1} \mid X_i = x_i, \theta = \theta_\eta) := K^{-1} \exp\Big[-\alpha\big(\delta\left(x_i, X_{i+1}, \theta_\eta\right) - \delta\left(x_i, \theta_\eta\right)\big)\Big]. \quad (1)$$

The normalising constant K is defined as

$$K = \sum_{x_{i+1} \in \chi^+} \Pr(X_{i+1} = x_{i+1} \mid X_i = x_i, \theta = \theta_\eta),$$

where $\chi^+ \subset \mathcal{X}$ is the set of all x_{i+1} that can be reached from x_i in one time step.

Figure 3 illustrates the two path distances in (1). This proposed model specifies that, for a given goal, movements that lead to shorter paths are more likely, while movements that result in longer paths are less likely. We wish to emphasise that this intuition is for a given goal and therefore it does not follow that the agent's intention is necessarily more likely to be a closer goal region than a further region.

The parameter α describes how likely the agent is to take the shortest path to the goal region. The value is constrained to $\alpha > 0$. As $\alpha \to \infty$, the agent will almost certainly take the shortest possible path to the goal. Conversely, as $\alpha \to 0$, all possible paths to the goal are equally likely. The most appropriate value of α may be selected based on training trajectories or vary according to other factors in the environment, such as the presence of other agents. In this paper we assume α is known and fixed, but we leave this open to future work.

IV. Bayesian Trajectory Prediction

We formulate a Bayesian estimation framework based on the graphical model in Fig. 2. At each timestep we first update an estimate of the intention θ and then use this to update the predicted future trajectory of the agent.

A. Joint Distribution

The probability distribution for the estimate of position X_{i+1} at time t_i is conditional on the previously observed position $X_i = x_i$ and the intention θ of the agent. From Fig. 2, the joint distribution of the probabilistic model is given as

$$\Pr(X_{1:i}, X_{i+1:i+k}, \theta) = \Pr(\theta) \prod_{j=1}^{i+k-1} \Pr(X_{j+1} \mid X_j, \theta).$$

B. Intention Inference

The probability distribution for the estimate of θ given the observed trajectory $x_{1:i}$ up to time t_i can be calculated using Bayes' theorem and applying the Markov assumption of the graphical model, such that the posterior is given by

$$\Pr(\theta \mid X_{1:i} = x_{1:i}) \propto \Pr(X_i = x_i \mid X_{i-1} = x_{i-1}, \theta) \times \Pr(\theta \mid X_{1:i-1} = x_{1:i-1}), \quad (2)$$

with a uniform initial distribution $\Pr(\theta \mid X_1 = x_1)$. The first factor in the right hand side of (2) is the likelihood of an observation and can be computed directly from the transition model (1). The second factor is the prior which is recursively updated as the previous posterior.

C. Trajectory Prediction

The future trajectory $X_{i+1:i+k}$ of the agent is predicted based on the current estimate for θ (2). This is achieved by marginalising the transition model (1) over θ, i.e. for 1

timestep into the future:

$$\Pr(X_{i+1} \mid X_{1:i} = x_{1:i}) = \sum_{\theta_\eta \in \Theta} \Big[\Pr(X_{i+1} \mid X_i = x_i, \theta = \theta_\eta) \times \Pr(\theta = \theta_\eta \mid X_{1:i} = x_{1:i}) \Big]. \quad (3)$$

The first factor in the right hand side can be computed directly from the transition model (1) and the second factor is the estimate of the intention (2).

This model is recursively extrapolated j timesteps into the future by marginalising over all possible unobserved trajectories at each timestep, yielding

$$\Pr(X_{i+j+1} \mid X_{1:i} = x_{1:i}) = \sum_{x_{i+j} \in \chi^-} \Big[\Pr(X_{i+j+1} \mid X_{i+j} = x_{i+j}) \times \Pr(X_{i+j} = x_{i+j} \mid X_{1:i} = x_{1:i}) \Big], \quad (4)$$

where the sum argument $x_{i+j} \in \chi^-$ denotes the set of all positions such that X_{i+j+1} is reachable from x_{i+j} in one time step. An analytical evaluation of (4) is difficult due to the exponential branching factor $|\chi|$ at each timestep. Therefore in the following section we propose a sampling technique which iteratively converges to the true distribution.

V. Sampling-Based Algorithm

In this section we propose an efficient algorithm that outputs probability distributions for the intention estimates and trajectory predictions based on the theoretical solution developed in the previous section. The algorithm begin by discretising the environment and the set of intentions using a graph representation. Prediction is performed after each position observation $X_i = x_i$, in two phases:

i. Update the estimate of the intention $\Pr(\theta \mid X_{1:i} = x_{1:i})$.
ii. Trajectory prediction by evaluating the distribution $\Pr(X_{i+j+1} \mid X_{1:i} = x_{1:i})$ using Monte-Carlo sampling.

An overview of the algorithm is shown in Alg. 1.

Algorithm 1 Trajectory prediction algorithm.

1: /* Precomputation */
2: $[\mathcal{V}, \mathcal{E}] \leftarrow$ GENERATE GRAPH (Ψ)
3: $\theta'_\eta \leftarrow \{v_i : v_i \in (\theta_\eta \cap \mathcal{V})\},\ \forall \theta_\eta \in \Theta$
4: $\mathcal{T}_{v_i} \leftarrow$ SPANNINGTREE$(\mathcal{V}, \mathcal{E}, v_i),\ \forall v_i \in \mathcal{V}$
5: $\delta(v_i, \theta'_\eta) \leftarrow$ SHORTDIST$(\mathcal{T}_{v_i}, \theta'_\eta),\ \forall v_i \in \mathcal{V}, \theta'_\eta \in \Theta'$
6: /* At each timestep */
7: **for each** t_i **do**
8: Observe $X_i = v_i$
9: /* Intention Inference */
10: **for each** $\theta_\eta \in \Theta$ **do**
11: $\Pr(X_i = v_i \mid X_{i-1} = v_{i-1}, \theta' = \theta'_\eta) \leftarrow (1)$
12: $\Pr(\theta = \theta_\eta \mid X_{1:i} = v_{1:i}) \leftarrow (2)$
13: **end for**
14: /* Trajectory Prediction */
15: $count(\hat{x}, j) \leftarrow 0,\ \forall \hat{x} \in \hat{\mathcal{X}},\ j \in \{i+1 : maxTime\}$
16: **for each** $\theta_\eta \in \Theta$ **do**
17: /* Draw N sample trajectories */
18: $N_\eta \leftarrow \Pr(\theta = \theta_\eta \mid X_{1:i} = v_{1:i}) \times N$
19: **for each** $n \in 1 : N_\eta$ **do**
20: $v_{i:b} \leftarrow$ DRAWSAMPLEPATH(v_i, θ'_η)
21: $x_{i+1:i+k} \leftarrow$ INTERPOLATE$(v_{i:b})$
22: /* Bin the samples at each time step */
23: **for each** $j \in 1 : k$ **do**
24: $\hat{x} \leftarrow$ ROUND(x_{i+j})
25: $count(\hat{x}, j) \leftarrow count(\hat{x}, j) + 1$
26: **end for**
27: **end for**
28: **end for**
29: $\Pr(X_j \in \hat{x} \mid X_{1:i} = v_{1:i}) \leftarrow \dfrac{count(\hat{x}, j)}{N},\ \forall \hat{x} \in \hat{\mathcal{X}},\ j \in \{i+1 : maxTime\}$
30: **end for**

A. Precomputation

1) Discrete Roadmap (line 2): For non-trivial problems, the theoretical equations are computable only when time is discretised and there exists a finite set of possible transitions at each timestep. We therefore discretise the environment Ψ into a discrete set of feasible positions $v_i \in \mathcal{V} \subseteq \mathcal{X}$ of the agent. Additionally, there is a finite set of feasible transitions $e_\eta = \langle v_i, v_j \rangle \in \mathcal{E}$ that describes moving from the position v_i to the position v_j in one timestep. The sets $(\mathcal{V}, \mathcal{E})$ describe the vertices and edges of a graph that gives a discrete roadmap representation of the environment. The graph should be formed such that any path through the environment can be sufficiently approximated by a path through the graph. For the examples used in this paper we utilise a probabilistic roadmap (PRM) formulation, however other roadmaps may also be considered.

2) Set of Intentions (line 3): The problem specification assumes there is a predefined finite set of possible goal regions $\theta_\eta \in \Theta$. In the graph representation, each region is represented by a set of vertices

$$\theta'_\eta := \{v_i : v_i \in (\theta_\eta \cap \mathcal{V})\}.$$

A trajectory to a goal region θ_η is represented as a path through the graph $(\mathcal{V}, \mathcal{E})$ that ends at any $v_i \in \theta'_\eta$.

3) Shortest-Path Distances (lines 4-5): The intention inference and the sampling both require repeatedly evaluating the shortest path distances from various vertices to all goals. It is therefore worth precomputing a database of shortest path distances from every vertex $v_i \in \mathcal{V}$ to every goal $\theta_\eta \in \Theta$. This can be achieved by building a shortest-path spanning tree $\mathcal{T}_{v_i}$ for every $v_i \in \mathcal{V}$ using an algorithm such as Dijkstra's (line 4). The distance $\delta(v_i, \theta_\eta)$ is evaluated as the distance to the closest $v_j \in \theta'_\eta$ as given by $\mathcal{T}_{v_i}$ (line 5). This process may be repeated $\forall v_i \in \mathcal{V}$ in parallel.

B. Intention Estimates (lines 10-13)

At every time step, the position of the agent is observed $X_i = x_i$ and the current vertex v_i is chosen as the $v_i \in \mathcal{V}$

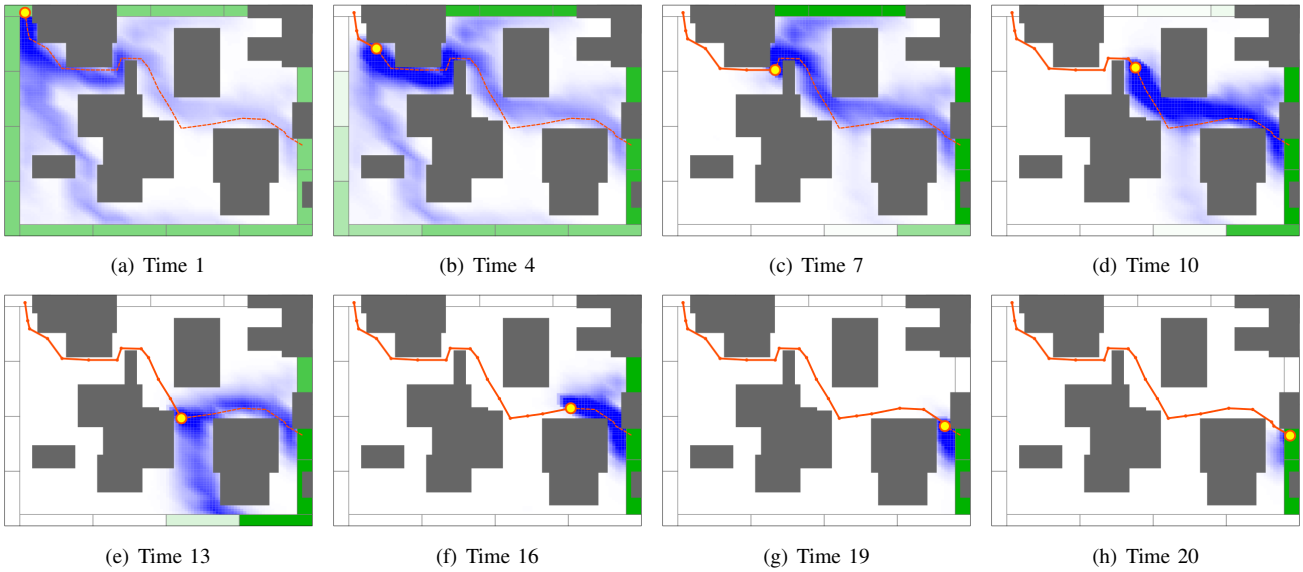

(a) Time 1 (b) Time 4 (c) Time 7 (d) Time 10

(e) Time 13 (f) Time 16 (g) Time 19 (h) Time 20

Fig. 4. Agent (orange) moving through a simulated environment with static obstacles (grey), from top left to middle right. There are 16 goal regions (green) evenly spaced around the boundary; dark goals have a high posterior probability while light goals have a low posterior probability. The path prediction is shown in blue; the shade of blue is proportional to the probability that $\hat{x}$ is visited by the agent at any time in the future. Note that this figure accumulates over all future time steps, while Fig. 5 depicts single timesteps in the future. The probabilities between adjacent cells have been interpolated.

which has the closest distance to x_i (line 8). This observation is used to update the intention estimate by directly evaluating and normalising (1) and (2) for each $\theta_\eta \in \Theta$.

C. Monte-Carlo Trajectory Prediction (lines 15-29)

The general solution for the trajectory prediction (4) is difficult to evaluate due to the branching factor $|\chi^+|$ of possible transitions at every step into the future. Therefore we propose a Monte-Carlo sampling technique that converges to the true distribution as more samples are drawn.

1) Cells (line 15): Firstly, the space $\mathcal{X}$ is partitioned into small cells $\hat{x} \in \hat{\mathcal{X}}$. The probability distribution $\Pr(X_j \mid X_{1:i} = x_{1:i})$ for a time t_j in the future will be estimated over these cells $\Pr(X_j \in \hat{x} \mid X_{1:i} = v_{1:i}),\ \forall \hat{x} \in \hat{\mathcal{X}}$. The partitioning structure and resolution may be chosen appropriately based on the application. The examples use a uniformly-spaced grid covering the environment.

2) Draw Sample Paths (lines 16-28): The sampling proceeds by drawing N sample trajectories from v_i to a goal θ_η. The number of samples N_η allocated to each θ_η is proportional to the posterior probability of $\theta = \theta_\eta$ (line 18). Note that each sample may be computed in parallel.

A sample path from v_i to θ'_η is drawn by recursively following edges $\langle v_i, v_j \rangle$, where each v_j is drawn from the probabilistic transition model distribution (1), given a fixed goal region θ'_η (line 20). In other words, sample paths are random walks over the graph that bias towards shorter paths to the goal region θ'_η. Given that the transition model specifies that shorter paths are more likely (for a given goal region), the recursion should always quickly reach θ'_η. However, an upper bound $|v_{i:b}| < U$ on the number of iterations before halting a path may be required for some environments, and is reasonable since most applications are only interested in predicting up to some fixed time horizon.

Each sample path $v_{i:b}$ is mapped to a sample trajectory defined as a set of positions $x_{i+1:i+k}$ at evenly spaced timesteps (line 21). This interpolation takes into account the probabilistic speed model by drawing from the velocity distribution distribution $|\dot{X}|$ given in the problem specification. It is assumed that after the agent reaches θ_η at time t_{i+k} it is no longer relevant, for example because it then moves beyond the boundary of the environment.

3) Trajectory Prediction Distributions (lines 23-29): For every $x_j \in x_{i+1:i+k}$ of a sample trajectory, the algorithm finds the cell $\hat{x}$ where $x_j \in \hat{x}$. A counter corresponding to the cell $\hat{x}$ and time t_j is incremented by 1 (line 25). Each counter represents the number of times that cell $\hat{x}$ is visited at time t_j by the N sample trajectories. The probability distribution at each time t_j in the future is therefore evaluated by dividing by the total number of samples (line 29).

D. Analysis

The estimated trajectory prediction distribution will converge towards the true distribution (4) as the number of vertices in the PRM increases and as the number of sample paths drawn for the sampling method increases. We empirically show convergence of the distribution as the number of samples increases in the experimental section.

The worst-case time complexity for the offline precomputation is cubic in the number of vertices of the PRM and the online trajectory prediction at each timestep is linear in the number of samples. More formally, we denote B as the maximum number of edges out of any vertex and R as the interpolation rate of the sample paths. The offline precomputation phase is dominated by building the spanning trees from all vertices which has complexity $\mathcal{O}(|\mathcal{V}|^3)$. Computation after each observation has complexity for: updating the posterior of the intention inference $\mathcal{O}(B|\Theta|)$,

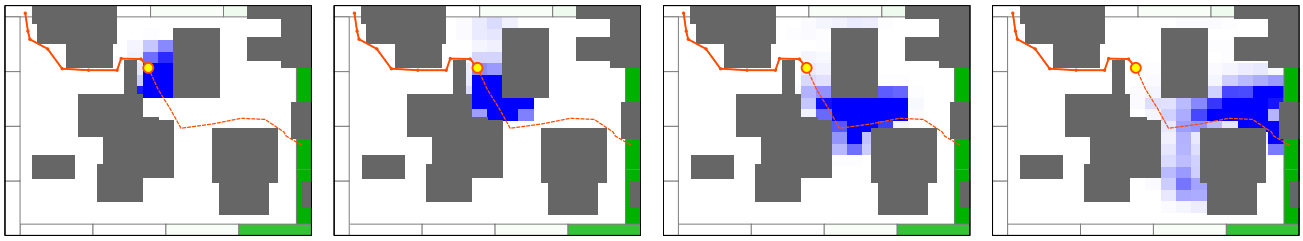

(a) Prediction for time 11 (b) Prediction for time 13 (c) Prediction for time 15 (d) Prediction for time 18

Fig. 5. Same trajectory prediction as shown in Fig. 4(d) (time 10); however the predicted position is shown for single timesteps in the future.

evaluating N sample paths $\mathcal{O}(N(BU + RU))$, evaluating the resulting prediction distributions $\mathcal{O}(|\hat{\mathcal{X}}|)$ and therefore a total complexity of $\mathcal{O}(B|\Theta| + N(BU + RU) + |\hat{\mathcal{X}}|)$, which in most cases will be dominated by $\mathcal{O}(NBU)$ since $|\Theta|$ and $|\hat{\mathcal{X}}|$ are typically smaller than N.

VI. Experiments

In this section we present experimental results to give an intuitive understanding of the algorithm, show its feasibility in practice for predicting human movements using a real-world pedestrian dataset and highlight advantages of the proposed intention inference concept over predictions that do not consider the agent's intention.

A. Simulated Environment

Figures 4(a)-(h) shows a simulated agent moving from top left to middle right through an environment with 16 goal regions around the boundary. Figure 4 shows the distribution of the trajectory prediction accumulated over all future timesteps, while Fig. 5 demonstrates how the algorithm gives probability distributions for individual timesteps in the future. The information shown in these figures can be used by another agent to avoid collisions with the dynamic agent who's trajectory is being predicted. The other agent should avoid the blue areas at particular times since otherwise there is some probability that a collision would occur.

We analyse the behaviour of the algorithm in this example as follows. (a) At time 1, the goal regions have a uniform prior and therefore the trajectory prediction almost covers the entire environment. (b) By time 4, the agent has started moving towards the right rather than downwards, and therefore the goal regions on the right side of the map now have a larger posterior probability and the trajectory has a higher density in this direction. (c) At time 7, the goal regions at the top and right of the map have a similar posterior probability, but the following movement (d) suggests that the top regions are unlikely. (e) The downward movement towards the centre suggests the agent is moving towards the bottom right, however it is not yet clear which direction it will move around the bottom right obstacle. (f)-(h) As the agent moves closer to the actual goal region, the predicted trajectory converges towards the actual trajectory. This increased certainty is due to the increasing posterior intention probability for the actual goal region. (h) At the end of the actual path, there is still some probability that the agent will continue moving downwards to the bottom right region.

Figure 5 shows the predicted position distribution at individual timesteps in the future from the same observed position as Fig. 4(d). These figures show how the uncertainty in position increases when extrapolating to timesteps further ahead in the future. For the purpose of dynamic-obstacle collision avoidance, the predictions presented in this form shows how the algorithm can be used to tell another agent the probability of a collision at a particular time and position.

In this example the environment was represented using a 1,000 vertices PRM with edges between all pairs of vertices that are straight line visible and have a distance less than one-tenth the width of the environment. The trajectory prediction used $\hat{X}$ chosen as a grid of 20×20 cells. Each prediction step used 1,000 sample paths, which takes approximately 500 ms. using un-optimised code and performed in parallel on a standard 4-core desktop processor. The distribution converges as more samples are taken, however with 1,000 samples the distribution has a mean squared error of 10^{-5} relative to a 100,000 sample distribution estimate for this example.

B. Real-World Pedestrian Dataset

We show the feasibility and advantages of the proposed trajectory prediction using intention inference by performing simulated experiments with 442 pedestrian trajectories from a real-world dataset by Lerner *et al.* [10][1]. The simulated environment is shown in Fig. 6 with 50 example pedestrian trajectories and 12 selected goal regions around the boundary. Each pedestrian either walked along the footpath through the middle, crossed the road at the bottom boundary while

[1]Dataset published at: `graphics.cs.ucy.ac.cy/research/downloads/crowd-data`

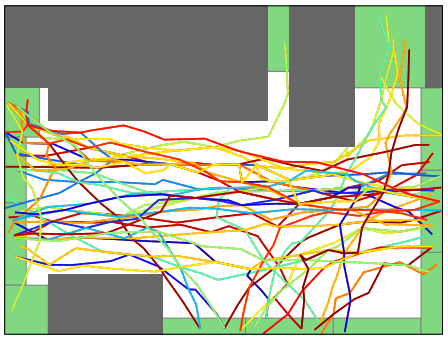

Fig. 6. The environment of the dataset with 50 example pedestrian trajectories and 12 selected goal regions.

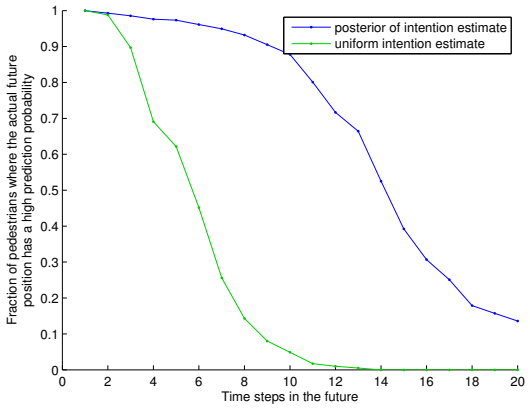

Fig. 7. Accuracy of the trajectory predictions for all pedestrian trajectories. Compares predicting with and without taking into account the intention estimate posterior. Vertical axis is the fraction of pedestrians that have a high prediction probability for the ground-truth future position of the agent. The predictions are made after 10 observed timesteps.

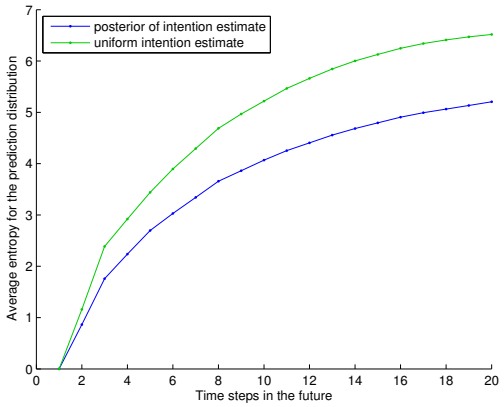

Fig. 8. Prediction uncertainty when predicting with and without taking into account the intention estimate posterior. Vertical axis is the entropy of the prediction distribution at each future timestep. Same conditions as Fig. 7.

avoiding the parked car, entered or exited the shop doorway in the top left, or walked down the driveways in the top right.

The accuracy of trajectory predictions averaged over all pedestrians is shown in Fig. 7. For timesteps near in the future, the algorithm most often gives a relatively high probability to the cell of the ground-truth future position. The probability threshold is set to $p(\hat{x}^*) > 0.05$, which may represent a safety threshold for a collision avoidance planner. The accuracy drops when looking further in the future since the uncertainty grows when extrapolating to future timesteps.

Figure 7 also shows that trajectory prediction with the posterior intention estimate outperforms predictions with a uniform intention estimate; a high accuracy is maintained for many more timesteps into the future. Intuitively, this is because the uniform case can only extrapolate outwards from the current position whereas the intention inference case directs predictions towards the estimated goal regions.

Figure 8 shows the uncertainty of the prediction distributions when using the posterior intention estimate results in distributions with lower entropy than the uniform case. This is important when applied to dynamic obstacle collision avoidance since a probabilistic planner has fewer cells that it must avoid and therefore has more freedom to find improved collision-free paths that satisfy other objectives.

VII. Conclusions

We have proposed a Bayesian framework for predicting the future trajectory of an agent by estimating its intention to move to a goal region in the environment, and have presented a computationally efficient solution. Our next step is to incorporate our method into motion planning algorithms. It is also important in future work to explore other types of intentions and objective functions, model interaction with other agents, and consider observation uncertainty.

Acknowledgements

This work is supported in part by the Australian Centre for Field Robotics and the NSW State Government. This research was also supported by funding from the Faculty of Engineering & Information Technologies, The University of Sydney, under the Faculty Research Cluster Program.

References

[1] G. S. Aoude, B. D. Luders, J. M. Joseph, N. Roy, and J. P. How. Probabilistically safe motion planning to avoid dynamic obstacles with uncertain motion patterns. *Auton. Robot.*, 35(1):51–76, 2013.

[2] T. Bandyopadhyay, K. Won, E. Frazzoli, D. Hsu, W. Lee, and D. Rus. Intention-aware motion planning. In *Proc. of WAFR*, 2012.

[3] G. Best, W. Martens, and R. Fitch. A spatiotemporal optimal stopping problem for mission monitoring with stationary viewpoints. In *Proc. of Robotics: Science and Systems*, 2015.

[4] A. Bruce and G. Gordon. Better motion prediction for people-tracking. In *Proc. of IEEE ICRA*, 2004.

[5] E. Charniak and R. P. Goldman. A bayesian model of plan recognition. *Artif. Intell.*, 64(1):53 – 79, 1993.

[6] H.-T. Chiang, N. Malone, K. Lesser, M. Oishi, and L. Tapia. Aggressive moving obstacle avoidance using a stochastic reachable set based potential field. In *Proc. of WAFR*, 2014.

[7] R. P. Goldman, C. W. Geib, and C. A. Miller. A new model of plan recognition. In *Proc. of AUAI UAI*, pages 245–254, 1999.

[8] A. Huntemann, E. Demeester, E. Poorten, H. Van Brussel, and J. De Schutter. Probabilistic approach to recognize local navigation plans by fusing past driving information with a personalized user model. In *Proc. of IEEE ICRA*, pages 4376–4383, 2013.

[9] S. Kim, S. J. Guy, W. Liu, D. Wilkie, R. W. Lau, M. C. Lin, and D. Manocha. Brvo: Predicting pedestrian trajectories using velocity-space reasoning. *Int. J. Robot. Res.*, 34(2):201–217, 2015.

[10] A. Lerner, Y. Chrysanthou, and D. Lischinski. Crowds by example. *Comput. Graph. Forum*, 26(3):655–664, 2007.

[11] S. Pellegrini, A. Ess, K. Schindler, and L. Van Gool. You'll never walk alone: Modeling social behavior for multi-target tracking. In *Proc. of IEEE ICCV*, pages 261–268, 2009.

[12] S. Reece and S. Roberts. The near constant acceleration gaussian process kernel for tracking. *IEEE Signal Proc. Let.*, 17(8):707–710, 2010.

[13] M. Schreier, V. Willert, and J. Adamy. Bayesian, maneuver-based, long-term trajectory prediction and criticality assessment for driver assistance systems. In *Proc. of IEEE ITSC*, pages 334–341, 2014.

[14] P. Trautman, J. Ma, R. Murray, and A. Krause. Robot navigation in dense human crowds: the case for cooperation. In *Proc. of IEEE ICRA*, pages 2153–2160, 2013.

[15] Z. Wang, K. Mlling, M. P. Deisenroth, H. Ben Amor, D. Vogt, B. Schlkopf, and J. Peters. Probabilistic movement modeling for intention inference in human-robot interaction. *Int. J. Robot. Res.*, 32(7):841–858, 2013.

[16] Z. Xu, R. Fitch, J. Underwood, and S. Sukkarieh. Decentralized coordinated tracking with mixed discrete-continuous decisions. *J. Field Robot.*, 30(5):717–740, 2013.

[17] K. Yamaguchi, A. Berg, L. Ortiz, and T. Berg. Who are you with and where are you going? In *Proc. of CVPR*, pages 1345–1352, 2011.